Extreme Hydraulic Gradient Statistics in Stochastic Earth Dam

By Gordon A. Fenton[1] and D. V. Griffiths,[2] Member, ASCE

ABSTRACT: The existence of large hydraulic gradients in regions of an earth dam where fine-grained soils are inadequately filtered can sometimes lead to internal erosion and piping failure. This paper investigates the stochastic nature of hydraulic gradients through two different earth dam cross sections, both with simple drains. In particular the magnitude and location of maximum hydraulic gradients are studied via Monte Carlo simulation to derive their probability distributions and assess their variability. These results can be used to guide designers with respect to minimizing the risk of internal erosion in the presence of uncertain soil permeability. The effect that the stochastic nature of the permeability field has on the hydraulic gradient distribution is compared to hydraulic gradients obtained in the deterministic case. This enables an evaluation of the importance of considering permeability randomness in the design process.

INTRODUCTION

Earth dams fail from a variety of causes. Some, such as earthquake or overtopping, may be probabilistically quantifiable through statistical analysis. Others, such as internal erosion, are mechanically complex, depending on internal hydraulic gradients, soil gradation, settlement fracturing, drain and filter performance, etc. In this paper the focus is on evaluating how internal hydraulic gradients are affected by spatial variability in soil permeability. The scope is limited to the study of simple, but reasonable, cases. Variability in internal hydraulic gradients is compared to traditional "deterministic" analyses in which the soil permeability is assumed constant throughout the earth dam cross section.

In a study of the internal stability of granular filters, Kenney and Lau (1985) state that grading stability depends on three factors: size distribution of particles, porosity, and severity of seepage and vibration. Most soil stability tests proceed by subjecting soil samples to prescribed gradients (or fluxes, or pressures) that are believed to be conservative, that is, which are considerably higher than believed "normal," as judged by current practice. For example, Kenney and Lau (1985) performed their soil tests using unit fluxes ranging from 0.48 to 1.67 cm/sec. Lafleur et al. (1989) used gradients ranging from 2.5 to 8.0, while Sherard et al. (1984a, 1984b) employed pressures ranging from 0.5 to 6 kg/cm² (corresponding to gradients up to 2,000). Mokenkamp et al. (1979) investigate the performance of filters under cyclically reversing hydraulic gradients. In all cases the tests are performed under what are believed to be conservative conditions.

By considering the soil permeability to be a spatially random field with reasonable statistics, it is instructive to investigate just how variable the gradient (or flux, or potential) can be at critical points in an earth dam. In this way the extent of conservatism in the aforementioned tests can be assessed. Essentially this paper addresses the question, "Should uncertainty about the permeability field be incorporated into the design process?" Or put another way, "Are deterministic design procedures sufficiently safe as they stand?" For example, if the internal gradient at a specific location in the dam has a reasonably high probability of exceeding the gradients under which soil stability tests were performed, then perhaps the use

of the test results to form design criteria needs to be reassessed.

The study will concentrate on the two earth dam cross sections shown in Fig. 1 with drains crosshatched. The steeper sloped dam will be referred to here as dam A and the shallower cross section as dam B. The overall dimensions of the dams were arbitrarily selected since the results are scalable (as explained later), only the overall shape being of importance.

The next two sections of the paper discuss the stochastic model—comprising random-field and finite-element models—used to represent the earth dam for the two geometries considered. In the "Downstream Free Surface Exit Elevation" section, the issue of how a simple internal drain—designed to avoid having the free surface exit on the downstream face of the dam above the drain—performs in the presence of spatially varying permeability. Successful drain performance is assumed to occur if the free surface remains contained within the drain at the downstream face with acceptably high probability.

The final section of the paper looks at the mean and standard deviation of internal hydraulic gradients. Gradients are defined here strictly in magnitude; direction is ignored. Again the dams are considered to have a drain in place. Regions where the gradients are highest are identified and the distribution of these maximum gradients established via simulation.

STOCHASTIC MODEL

The stochastic model used to represent flow through an earth dam with free surface is an extension of the model re-
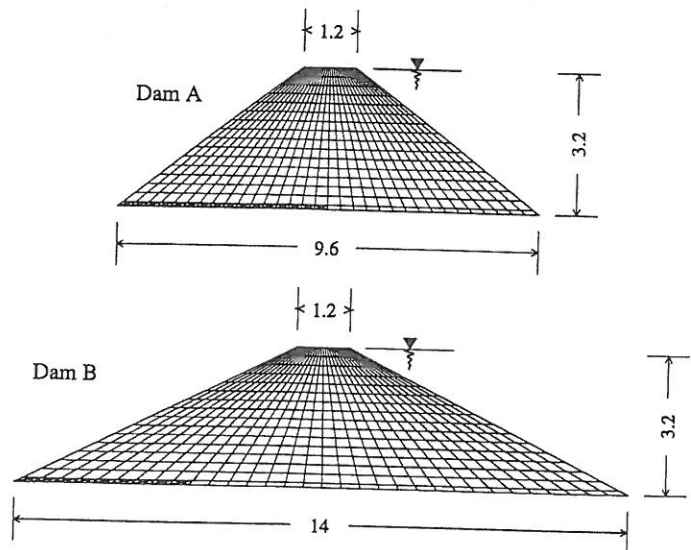
[1]Assoc. Prof., Dalhousie Univ., Halifax, NS, B3J 2X4, Canada.
[2]Prof., Colorado School of Mines, Golden, CO 80401.

FIG. 1. Two Earth Dam Geometries Considered in Stochastic Analysis

ported by Fenton and Griffiths (1996). When the permeability is viewed as a spatially random field, the equations governing the flow become stochastic. The random field characterizes uncertainty about the permeability at all points in the dam and from dam to dam. The flow through the dam will thus also be uncertain and this uncertainty can be expressed by considering the probability distribution of various quantities related to flow.

The permeability, $K(\underline{x})$, is assumed to follow a lognormal distribution, consistent with the findings of Freeze (1975), Hoeksema and Kitanidis (1985), and Sudicky (1986) and with the work of Griffiths and Fenton (1993), with mean μ_k and variance σ_k^2. Thus $\ln K$ is normally distributed (Gaussian) with mean $\mu_{\ln k}$ and variance $\sigma_{\ln k}^2$, where

$$\sigma_{\ln k}^2 = \ln\left(1 + \frac{\sigma_k^2}{\mu_k^2}\right); \quad \mu_{\ln k} = \ln(\mu_k) - \frac{1}{2}\sigma_{\ln k}^2 \quad (1a,b)$$

Since $K(\underline{x})$ is a spatially varying random field, there will also be a degree of correlation between $K(\underline{x})$ and $K(\underline{x}')$, where $\underline{x}$ and $\underline{x}'$ are any two points in the field. Intuitively it makes sense that the permeability at $\underline{x}$ and $\underline{x}'$ will be similar if $\underline{x}$ and $\underline{x}'$ are close together. Alternatively if the two points are widely separated less correlation may be expected. Mathematically this concept is captured through the use of a spatial correlation function, which, in this study, is an exponentially decaying function of separation distance $\underline{\tau} = \underline{x} - \underline{x}'$ (Sudicky 1986)

$$\rho(\underline{\tau}) = e^{-2|\underline{\tau}|/\theta_{\ln k}} \quad (2)$$

where $\theta_{\ln k}$ is called the scale of fluctuation and governs the decay rate of correlation between points in the permeability field as a function of the distance between them. Loosely speaking the scale of fluctuation can be thought of as the distance over which points on the random field show substantial correlation. Eq. (2) is a Gauss-Markov model for which short scales of fluctuation yield "rougher" or less correlated fields, while longer scales yield smoother or more correlated fields. When $\theta_{\ln k} \to \infty$ the random field becomes completely correlated; all points on the field have the same permeability, assuming stationary mean, and variation only occurs from realization to realization (the permeability is still random, just not within a specific realization). When $\theta_{\ln k} = 0$ the permeabilities at all points become independent, a physically unrealizable situation. In fact, scales of fluctuation less than the size of laboratory samples used to estimate permeability have little meaning since Darcy's law is a continuum representation where the permeability is measured at the laboratory scale.

Simulation of the soil permeability field proceeds in two steps: first an underlying Gaussian random field, $Z(\underline{x})$, is generated with mean zero, unit variance, and spatial correlation function (2) using the local average subdivision (LAS) method introduced by Fenton and Vanmarcke (1990). The LAS algorithm produces a rectangular grid of elements, each element having a value assigned to it equal to the local average of the enclosed random field. This approach is well suited to use with finite-element analyses since local average values can be easily mapped to the finite elements and element statistics are properly related to the element size [as the element size increases the local average variance decreases due to the averaging effect, see Vanmarcke (1984)].

Next, since the permeability is assumed to be lognormally distributed, values of K_i, where i denotes the ith element, are obtained through the transformation

$$K_i = \exp\left[\mu_{\ln k} + \sigma_{\ln k} Z(\underline{x}_i)\right] \quad (3)$$

where $\underline{x}_i$ = centroid of the ith element; and $Z(\underline{x}_i)$ = local average value generated by the LAS algorithm of the cell within which $\underline{x}_i$ falls. The finite-element mesh is deformed while iterating to find the free surface so that local average elements

only approximately match the finite elements in area. Thus for a given realization the spatially "fixed" permeability field values are assigned to individual elements according to where the element is located on each free-surface iteration.

Both permeability and scale of fluctuation are assumed to be isotropic in this study. Although layered construction of an earth dam may lead to some anisotropy relating to the scale of fluctuation and permeability, this initial study employs the simpler isotropic mode. In addition the model itself is two-dimensional (2D), which is equivalent to assuming that streamlines remain in the plane of analysis. This will occur if the dam ends are impervious and if the scale of fluctuation in the out-of-plane direction is infinite (implying that soil properties are constant in the out-of-plane direction). Clearly the latter condition will be false; however, a full three-dimensional analysis is beyond the scope of the present study. It is believed that the 2D analysis will still yield valuable insights to the problem, as indicated by Griffiths and Fenton (1997).

Statistics of the output quantities of interest are obtained by Monte Carlo simulation employing 5,000 realizations of the soil permeability field for each cross section considered. With this number of independent realizations, estimates of the mean and standard deviations of output quantities of interest have themselves standard deviations of approximately

$$s_{m_X} \simeq \sqrt{\frac{1}{n}}\, s_X = 0.014 s_X; \quad s_{s_X^2} \simeq \sqrt{\frac{2}{n-1}}\, s_X^2 = 0.02 s_X^2 \quad (4a,b)$$

where X = output quantity of interest; m_X is its estimated mean; s_X is its estimated standard deviation; and s_{m_X} and $s_{s_X^2}$ are the estimated standard deviations of the estimators m_X and s_X, respectively.

Many of the statistical quantities discussed in the following are compared to the so-called deterministic case. The deterministic case corresponds to the traditional analysis approach in which the permeability is taken to be constant throughout the dam; here the deterministic permeability is equal to $\mu_k = 1.0$. For all stochastic analyses the permeability coefficient of variation (C.O.V.) is taken to be 0.50 and the scale of fluctuation is taken to be 1.0. These numbers are not excessive and are believed typical for a well-controlled earth dam fill.

FINITE-ELEMENT MODEL

For a given permeability field realization, the free surface location and flow through the earth dam are computed using a 2D iterative finite-element model derived from Smith and Griffiths (1988), Program 7.1. The elements are four-node quadrilaterals and the mesh is deformed on each iteration until the total head along the free surface approaches its elevation head above a predefined horizontal datum. Convergence is obtained when the maximum relative change in the free surface elevation at the surface nodes becomes less than 0.005. Fig. 2 illustrates two possible free surface profiles for dam B corresponding to different permeability field realizations with the same input statistics. Lighter regions on the figure correspond to higher permeabilities. Along the base of the dam, from the downstream face to the dam centerline, a drain is provided with fixed (nonrandom) permeability of 120 times the mean dam permeability. This permeability was selected to ensure that the free surface did not exit the downstream face above the drain for either cross section under deterministic conditions (constant permeability of $\mu_k = 1$ everywhere). It is assumed that this would be ensured in the normal course of a design. Notice that the drain itself is only approximately represented along its upper boundary because the elements are deforming during the iterations. This leads to some randomness in the drain behavior that, although not strictly quantifiable, may actually be quite realistic.

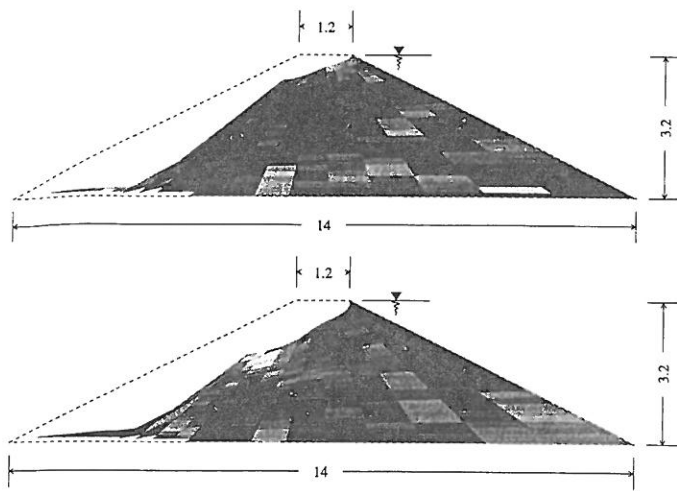In both cross sections the free surface is seen to fall into

FIG. 2. Two Possible Free Surface Realizations in Dam B

the drain, although not as fast as classical free surface profiles with drains would suggest. The difference here is that the drain has finite permeability; this leads to some back pressure causing the free surface to remain above it over some length. In that drains that also act as filters will not be infinitely permeable, these free surfaces are believed to be representative.

Since the finite-element mesh is moving during the iterative analysis, the gradients must be calculated at fixed points rather than at the nodal locations. This means that gradients must be interpolated using the finite-element shape functions once the element enclosing an arbitrary fixed point is identified. Thus, two meshes are carried throughout the analysis; one fixed and one deforming according to the free surface profile.

For each realization the computer program computes the following quantities:

- The free surface profile.
- The gradient, unit flux, and head at each point on a fixed lattice discretization of the dam cross section. Points that lie above the free surface for this particular realization are assigned a gradient of zero. Gradients are computed as

$$g = \sqrt{\left(\frac{\partial \phi}{\partial x_1}\right)^2 + \left(\frac{\partial \phi}{\partial x_2}\right)^2} \qquad (5)$$

which is the absolute magnitude of the gradient vector. The vector direction is ignored.
- Total flow rate through the cross section.

All quantities form part of a statistical analysis by suitably averaging over the ensemble of realizations.

In Fig. 1 the drains are denoted by crosshatching and can be seen to lie along the downstream dam base. The dams are discretized into 32 × 16 elements and the drain has thickness of 0.1 in the original discretization. In dam A the drain extends to the midpoint, while in dam B the drain has length 4, both measured from the downstream dam corner. The original, or undeformed, discretization shown in Fig. 1 is also taken to be the fixed discretization over which gradients are obtained.

Elements falling within the domain of the drain during the analysis are assigned a permeability of $120\mu_k$, the remainder assigned random permeabilities as discussed in the previous section. As also mentioned previously the elements in the deformed mesh are not rectangular so the drain is only approximated. Some elements lying above the drain have portions extending into the drain and vice versa. The permeability mapping algorithm has been devised to ensure that the drain itself is never "blocked" by portions of a low permeability element

extending into the drain. Given the uncertainty related to the infiltration of core fines into the drain, this model is deemed to be a reasonable approximation.

The overall dimensions of the dam and the assumed permeability statistics are scalable; that is, a dam having 10 times the dimensions of dam A or B will have 10 times the total flow rate, the same free surface profile, and the same gradients if both have the same (space scaled) permeability field. Output statistics are preserved if the prescribed scale of fluctuation is scaled by the same amount as the dam itself and the permeability mean and variance are unchanged. Regarding changes in the mean permeability, if the coefficient of variation (C.O.V. = σ_k/μ_k) remains fixed, then scaling μ_k results in a linear change in the flow rate (with unchanged C.O.V.) and unchanged gradient, and free surface profile statistics. The unit flux scales linearly with the permeability but is unaffected by changes in the dam dimension. The potential field scales linearly with the dam dimension, but is unaffected by the permeability field (as long as the latter also scales with the dam dimension).

DOWNSTREAM FREE SURFACE EXIT ELEVATION

The drain is commonly provided to ensure that the free surface does not exit on the downstream face of the dam, resulting in its erosion. The lowering of the free surface by this means will be referred to herein as "drawdown." As long as the drawdown results in an exit point within the drain itself, the drain can be considered to be performing acceptably. Fig. 3 shows the deterministic free surface profile for the two geometries considered. In both cases the free surface descends into the drain prior to reaching the downstream face.

Fig. 4 shows histograms of free surface exit elevations, Y, which are normalized with respect to the earth dam height. The dashed line is a normal distribution fitted to the data, with parameters given in the line key. For the cases considered the normalized dimension of the top of the drain is $0.1/3.2 = 0.031$, so there appears to be little danger of the free surface exiting above the drain when the soil is spatially variable, at least under the moderate levels of variability considered here. The normalized free surface exit elevations obtained in the deterministic case (uniform permeability) are 0.024 for dam A and 0.015 for dam B. The mean values obtained from the simulation, as indicated in Fig. 4, are 0.012 for dam A and 0.009 for dam B. Thus, the net effect of soil variability is to reduce the exit point elevation. Perhaps the major reason for this reduction arises from the length of the drain—in the pres-
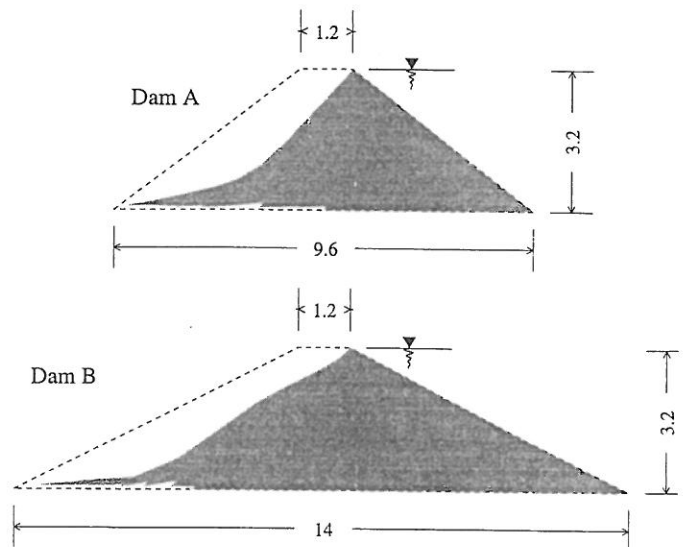

FIG. 3. Deterministic Free Surface Profiles

ence of spatial variability there exits a higher probability that somewhere farther along the drain the core permeability will be lower, tending to drive the flow into the drain. The deterministic flow rates (normalized with respect to μ_k), are 1.94 for dam A and 1.03 for dam B. The corresponding mean flow rates determined by simulation are somewhat reduced at 1.85 and 0.96, illustrating again that spatial variability tends to introduce "blockages" somewhere along the flow path. Since the C.O.V of the height of the free surface exit point is only around 15–17% for both cross sections, permeability spatial variability primarily serves to lower the exit point height, re-
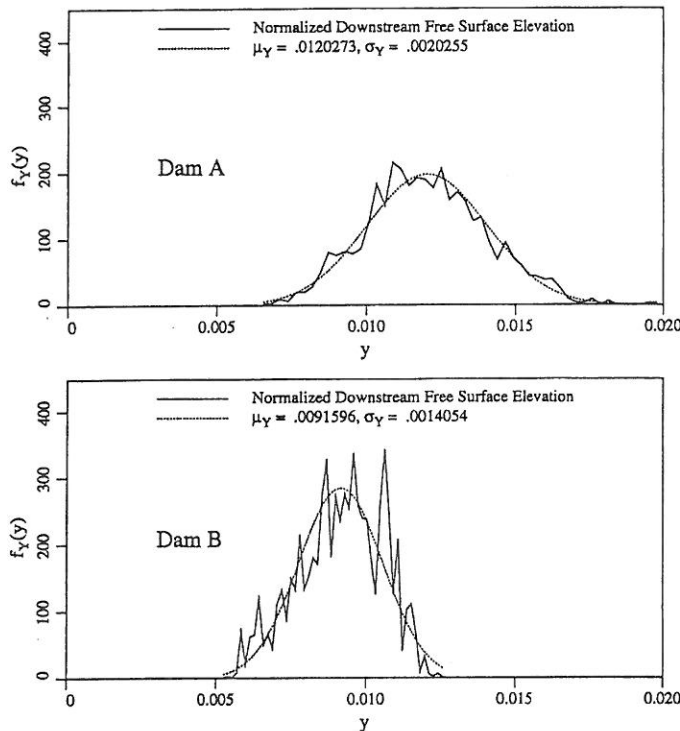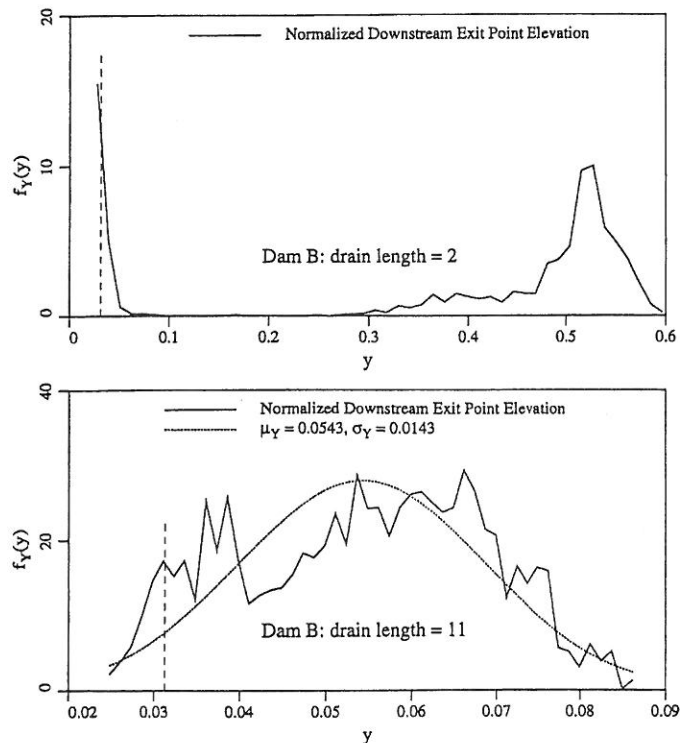
ducing risk of surface erosion, and does not result in signif[icant] variability in the exit point elevation, at least under th[e] input statistics assumed for these models. As will be seen late[r] the internal free surface profile has somewhat more variabilit[y]. However, this is not a design problem as it does not lead t[o] emergence of the free surface on the downstream face of th[e] core unless the drain is excessively short.

To investigate the effect of the drain length on the down[stream] stream exit elevation, the simulations for dam B (the shallow[er] dam) were rerun for drain lengths of 2.0 and 11.0. The resul[ts] are shown in Fig. 5, which includes the location of the no[r]malized drain height as a vertical dashed line. For the short[er] drain length the free surface exit point becomes bimodal, a[s] perhaps expected. A deterministic analysis with the short drai[n] predicts the free surface to exit at about the half height of th[e] dam. Occasionally realizations of the stochastic permeabili[ty] field provide a high permeability path to the drain and the fre[e] surface "jumps down" to exit through the drain rather tha[n] the downstream face. When the drain is extended a significan[t] distance into the dam, the total flow rate increases significant[ly] and the drain begins to approach its flow capacity. In this cas[e] the response of the dam overlying the drain approaches tha[t] of the dam without a drain and the free surface exit elevatio[n] rises. (For a drain length of 11.0 only about 10% of realiza[-] tions resulted in the free surface exiting within the drain[.]) Again, this response is predicted by the deterministic analysi[s].

In summary, the free surface exit elevation tends to hav[e] only a very small probability of exceeding the exit point ele[-] vation predicted by a deterministic analysis, implying that [a] deterministic analysis is conservative in this respect. Howeve[r] if the drain becomes "plugged" due to infiltration of fine[s] perhaps effectively reducing its length, then the free surfac[e] may "jump" to the downstream face and in general has [a] higher probability of exiting somewhere (usually around mi[d] height) on the downstream face. On the basis of these simu[-] lations it appears that if the drain is behaving satisfactoril[y] according to a deterministic analysis, then it will also behav[e] satisfactorily in the presence of spatially random permeabilit[y] assuming that the permeability mean and variance are reason[-] ably well approximated.

INTERNAL GRADIENTS

Fig. 6 shows a greyscale representation of the average in[-] ternal gradients, with dark regions corresponding to higher av[-] erage gradients. Clearly the highest average gradients occur a[t] the head of the drain (upper right corner), as expected.

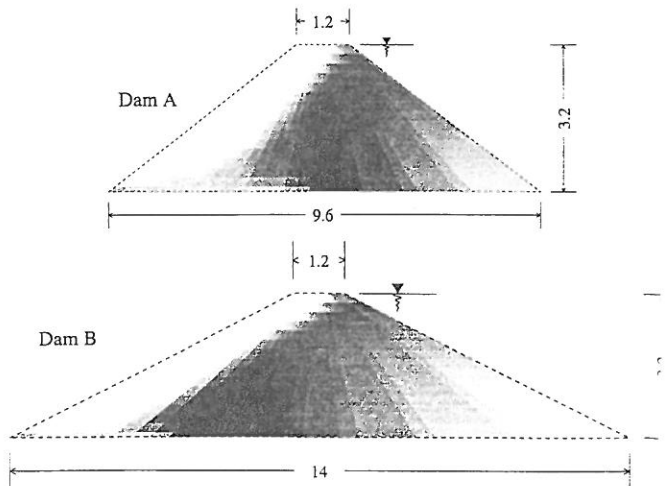Approaching the downstream face of the dam, the averag[e]

FIG. 4. Normalized Free Surface Exit Elevation

FIG. 5. Effect of Drain Length on Free Surface Exit Elevation

FIG. 6. Average Hydraulic Gradient Fields (High Gradients Ar[e] Dark)

internal gradients tend to fade out slowly. This reflects two things: (1) the gradients near the free surface tend to be small; and (2) the free surface changes location from realization to realization so that the average includes cases where the gradient is zero (above the free surface). The free surface itself sometimes comes quite close to the downstream face, but it always (with very high probability) descends to exit within the drain for the cases shown.

Fig. 7 shows a greyscale representation of the gradient standard deviation. Interestingly, larger standard deviations occur in the region of the mean free surface, as indicated by the dark band running along parallel to the downstream face, as well as near the head of the drain.

Clearly, the area near the head of the drain is where the maximum gradients occur, so this area has the largest potential for soil degradation and piping. The gradient distribution, as extracted from the finite-element program, at the drain head is shown in Fig. 8. The gradients observed in dam A extend all the way up to about 3.5, which is in the range of the soil tests
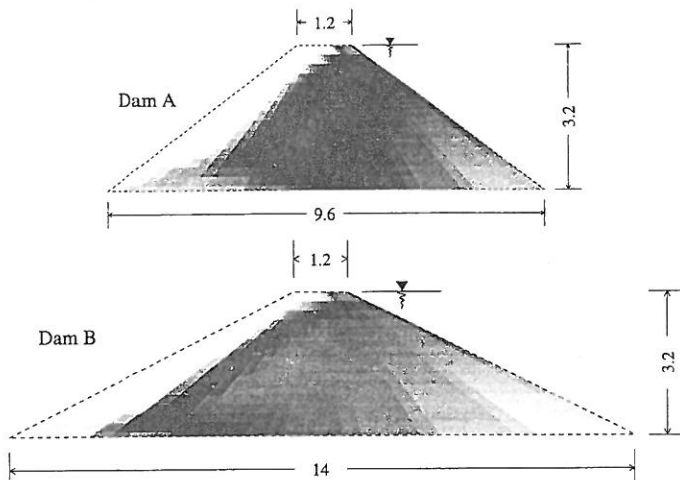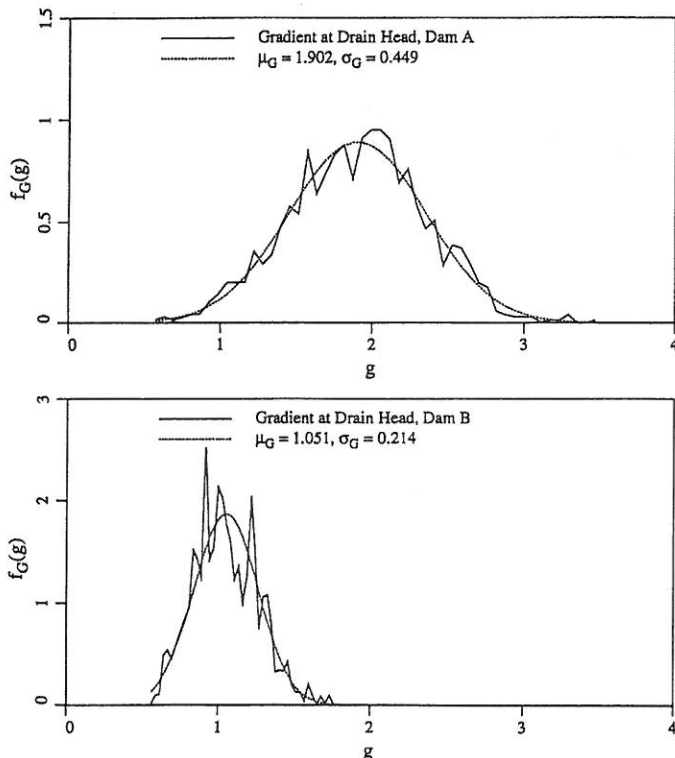
performed by Lafleur et al. (1989) on the filtration stability of broadly graded cohesionless soils. Thus it would appear that those test results, at least, cover the range of gradients observed in this dam. The wider dam B profile has a smaller range and lower gradients at the head of the drain, and so should be safer with respect to piping failure.

The deterministic gradients at the head of the drain were 1.85 for dam A and 1.08 for dam B. These values are very close to the mean gradients observed in Fig. 8, but imply that the deterministic result is not a conservative measure of the gradients possible in the region of the drain. The C.O.V.'s of the drain head gradients were 0.24 for dam A and 0.20 for dam B. Thus a ballpark estimate of the maximum gradient distribution for dams such as these might be to take the deterministic gradient as a mean and apply a C.O.V. of 25% under an assumed normal distribution. These results can be considered representative of any dam having one of these overall shapes with $\sigma_k/\mu_k = 0.5$ since the gradient is not affected by changing mean permeability or overall dam dimension.

For comparison, the unit flux near the head of the drain has distribution similar to that of the gradient with mean $1.77\mu_k$ and coefficient of variation of 0.36 for dam A. For the shallower dam B, the mean flux at the head of the drain is $1.02\mu_k$ with C.O.V. of 0.33. Although these results are not directly comparable with the stability tests carried out by Kenney and Lau (1985) under unit fluxes ranging from 0.48 to 1.67 cm/sec (they did not report the corresponding permeability), it seems likely that the soil samples they were testing would have permeabilities much smaller than 1.0. In this case the unit fluxes obtained in this simulation study are (probably) much smaller than those used in the test conditions, indicating again that the test conditions are conservative.

CONCLUSIONS

The primary conclusions derived from this study are as follows:

1. The downstream exit point elevation obtained using a deterministic analysis (constant permeability) is a conservative estimate. That is, the effect of spatial variability in the permeability field serves to lower the mean exit point elevation (as it does the mean flow rate).
2. The spatial variability of soil permeability does not significantly add variability to the free surface location. The exception to this occurs when a sufficiently short drain is provided that keeps the free surface so close to the downstream dam face that it "jumps" to exit on the downstream face under slight changes of the permeability field in the region of the drain. In general, however, for a sufficiently long and clear drain (somewhere between 1/4 and 1/2 the base dimension) the free surface profile is fairly stable. This observation has also been made in the absence of a drain (Fenton and Griffiths 1996), even though the profile in that case is much higher.
3. A drain having permeability at least 120 times the mean permeability of the dam itself and having length between 1/4 and 1/2 of the base dimension was found to be successful in ensuring that the downstream free surface exit point was consistently contained within the drain, despite variability in the permeability field. Specifically, the mean downstream exit point elevation was found to lie well within the drain. As noted above the exit point elevation has relatively small standard deviation (C.O.V. of less than 17%) so that the entire sample distribution also remained well within the drain.
4. Maximum internal hydraulic gradients occur near the

FIG. 7. Hydraulic Gradient Standard Deviation Fields (High Standard Deviations Are Dark)

FIG. 8. Hydraulic Gradient Distributions at Drain Heads

head of the drain (upstream end), and although there is more variability in the gradient field than in the free surface profile, the gradient distribution is not excessively wide. Coefficients of variation remain around 25% for both earth dam geometries considered (for an input C.O.V. of 50% on the permeability).

5. There does not seem to be any significant probability that spatial variability in the permeability field will lead to hydraulic gradients exceeding those values used in tests leading to soil stability design criteria. Thus design criteria based on published test results appears to be conservative, at least when considering only the influence of spatially varying permeability.

6. The hydraulic gradient distribution near the head of the drain has a mean very close to that predicted by a deterministic analysis with $K = \mu_k$ everywhere. A coefficient of variation of 25% can then be applied using a normal distribution to obtain a reasonable approximation to the gradient distribution.

Although these observations imply that existing design procedures based on "conservative" and deterministic tests do appear to be conservative and so can be used for drain design without regard to stochasticity, it must be emphasized that only one source of uncertainty was considered in this analysis under a single input C.O.V. A more complete (and complex) study would include soil particle distributions and differential settlements, and allow for particle movement, formation of preferential flow paths, drain blockage, etc. The results of this initial study are, however, encouraging, in that the stability design of the soil only considers soil gradation issues under vibration and seepage, and does not specifically account for larger scale factors such as differential settlement. What this means is that the results of this paper are useful if the dam behaves as it was designed, without formation of large cracks due to settlement or preferential flow paths, and without drain blockage, etc., and suggest that such a design would be conservative without the need to explicitly consider stochastic variation in the soil permeability.

ACKNOWLEDGMENTS

APPENDIX I.   REFERENCES

Fenton, G. A., and Griffiths, D. V. (1996). "Statistics of free surface flow through stochastic earth dam." ASCE, *J. Geotech. Engrg.*, 122(6), 427–436.

Fenton, G. A., and Vanmarcke, E. H. (1990). "Simulation of random fields via local average subdivision." ASCE, *J. Engrg. Mech.*, 116(8), 1733–1749.

Freeze, R. A. (1975). "A stochastic-conceptual analysis of one-dimensional groundwater flow in nonuniform homogeneous media." *Water Resour. Res.*, 11(5), 725–741.

Griffiths, D. V., and Fenton, G. A. (1993). "Seepage beneath water retaining structures founded on spatially random soil." *Géotechnique*, 43(4), 577–587.

Griffiths, D. V., and Fenton, G. A. (1997). "Three-dimensional seepage through spatially random soil." ASCE, *J. Geotech. Engrg.*, 123(2), 153–160.

Hoeksema, R. J., and Kitanidis, P. K. (1985). "Analysis of the spatial structure of properties of selected aquifers." *Water Resour. Res.*, 21(4), 563–572.

Kenney, T. C., and Lau, D. (1985). "Internal stability of granular filters." *Can. Geotech. J.*, Ottawa, Canada, 22(2), 215–225.

Lafleur, J., Mlynarek, J., and Rollin, A. L. (1989). "Filtration of broadly graded cohesionless soils." ASCE, *J. Geotech. Engrg.*, 115(12), 1747–1768.

Molenkamp, F., Calle, E. O., Heusdens, J. J., and Koenders, M. A. (1979). "Cyclic filter tests in a triaxial cell." *Proc., 7th European Conf. on Soil Mech. and Foundation Engrg.*, British Geotech. Soc., London, U.K., 97–101.

Sherard, J. L., Dunnigan, L. P., and Talbot, J. R. (1984a). "Filters for silts and clays." ASCE, *J. Geotech. Engrg.*, 110(6), 701–718.

Sherard, J. L., Dunnigan, L. P., and Talbot, J. R. (1984b). "Basic properties of sand and gravel filters." ASCE, *J. Geotech. Engrg.*, 110(6), 684–700.

Smith, I. M., and Griffiths, D. V. (1988). *Programming the finite element method*. John Wiley & Sons, New York, N.Y.

Sudicky, E. A. (1986). "A natural gradient experiment on solute transport in a sand aquifer: spatial variability of hydraulic conductivity and its role in the dispersion process." *Water Resour. Res.*, 22(13), 2069–2083.

Vanmarcke, E. H. (1984). *Random fields: analysis and synthesis*. The MIT Press, Cambridge, Mass.

APPENDIX II.   NOTATION

The following symbols are used in this paper:

$f_x(x)$ = probability density function of random variable X;
g = gradient magnitude;
K = permeability;
K_i = permeability associated with element i;
m_x = estimated mean of random variable X;
s_{m_x} = estimated standard deviation of the estimator m_x;
$s_{s_x^2}$ = estimated standard deviation of the estimator s_x^2;
s_x^2 = estimated variance of random variable X;
$\underset{\sim}{x}$ = spatial coordinate, $\{x_1, x_2\}$;
$\underset{\sim}{Y}$ = normalized exit point elevation (with realization y);
$Z(\underset{\sim}{x}_i)$ = mean zero, unit variance, Gaussian random field;
$\theta_{\ln k}$ = scale of fluctuation;
μ_k = mean permeability;
$\mu_{\ln k}$ = mean of log-permeability;
$\rho(\underset{\sim}{\tau})$ = spatial correlation function;
σ_k^2 = permeability variance;
$\sigma_{\ln k}$ = standard deviation of log-permeability;
$\sigma_{\ln k}^2$ = variance of log-permeability;
$\underset{\sim}{\tau}$ = separation vector; and
ϕ = hydraulic head.